Molecular Medicine 4: 217-230, 1998

Molecular Medicine

Original Articles

MIF Expression in the Rat Brain: Implications for Neuronal Function

Michael Bacher,[1] Andreas Meinhardt,[2] Hui Y. Lan,[3] Firdaus S. Dhabhar,[4] Wei Mu,[3] Christine N. Metz,[1] Jason A. Chesney,[1] Diethard Gemsa,[5] Thomas Donnelly,[1] Robert C. Atkins,[3] and Richard Bucala[1]

[1]The Picower Institute for Medical Research, Manhasset, New York, U.S.A.
[2]Institute of Reproduction and Development and
[3]Department of Nephrology, Monash Medical Centre, Clayton, Victoria, Australia
[4]Laboratory for Neuroendocrinology, Rockefeller University, New York, New York, U.S.A.
[5]Institute for Immunology, Philipps-University, Marburg, Germany

Communicated by R. Bucala. Accepted February 15, 1998.

Abstract

Background: The mediator known historically as macrophage migration inhibitory factor (MIF) has been identified recently as being released into the circulation by the anterior pituitary gland as a consequence of stress or during a systemic inflammatory response. Macrophages and T cells also secrete MIF, both in response to proinflammatory factors or upon stimulation with glucocorticoids. Once released, MIF "overrides" or counterregulates the immunosuppressive effects of steroids on cytokine production and immune cellular activation. To further investigate the biology of MIF and its role in the neuroendocrine system, we have studied the regional and cellular expression of MIF in brain tissue obtained from normal rats and rats administered LPS intracisternally.

Materials and Methods: Rat brain sections were analyzed by immunohistochemistry utilizing an affinity-purified, anti-MIF antibody raised to recombinant MIF, and by in situ hybridization using a digoxigenin-labeled, antisense MIF cRNA probe. The kinetics of MIF mRNA expression in brain were compared with that of IL-1, IL-6, and TNF-α by RT-PCR of total brain RNA. The cerebrospinal fluid content of MIF and TNF-α proteins was analyzed by Western blotting and ELISA.

Results: A strong baseline expression pattern for MIF was observed in neurons of the cortex, hypothalamus, hippocampus, cerebellum, and pons. By in situ hybridization, MIF mRNA was found predominantly in cell bodies whereas MIF protein was detected mostly within the terminal fields associated with neurons. There was a marked pattern of MIF immunoreactivity within the mossy fibers of the dentate gyrus and dendrites of the hippocampal CA3 field. These structures have been shown previously to be involved in glucocorticoid-induced tissue damage within the hippocampus, suggesting an association between MIF and targets of glucocorticoid action. The intracisternal injection of LPS increased MIF mRNA and protein expression in brain and MIF immunoreactivity was due in part to infiltrating monocytes/macrophages. MIF protein also was found to be rapidly released into the cerebrospinal fluid. This response corresponded with that of LPS-induced cytokine release and MIF mRNA expression increased in a distribution that colocalized in large part with that of TNF-α, IL-1β, and IL-6.

Conclusion: The significant levels of baseline and inducible MIF expression in the brain and its regional association with glucocorticoid action underscore the importance of this mediator as a physiological regulator of the inflammatory stress response and further define its role within the neuroendocrine system.

Introduction

The protein mediator known as macrophage migration inhibitory factor (MIF) was one of the first cytokine activities to be discovered and was described 30 years ago as a T cell–derived factor that inhibited the random migration of macrophages (1–3). More recent studies have led to the description of a pituitary mediator that appears to act as an endogenous, counterregulatory hormone for glucocorticoid action within the immune system. Isolated as a product of an anterior pituitary cell line, this protein was sequenced and found to be the mouse homolog of MIF (4). Subsequent work showed that macrophages and T cells secrete MIF in response to glucocorticoids and activation by proinflammatory stimuli (5,6). Once released, MIF can "override" the immunosuppressive effects of steroids on cytokine production and cellular activation. Since glucocorticoids are an integral component of the host reaction to invasive stimuli, it has become evident that MIF can act at an inflammatory site or lymph node to counterbalance the inhibitory effects of steroids on the primary immune response that must necessarily be mounted to eliminate the source of infection or tissue invasion.

Despite evidence establishing a critical function for MIF in the immune and inflammatory responses, emerging data have also identified MIF as an important component of the endocrine system and the hypothalamic–pituitary–adrenal (HPA) axis. Western and Northern analyses have shown MIF to be expressed constitutively by the anterior lobe of the pituitary gland and to be released into the circulation as a consequence of stress or inflammatory stimuli (4,6). Immunogold electron microscopy studies have shown that MIF is secreted from the same pituitary cell granules as those containing adrenocorticotropic hormone (ACTH) and thyroid-stimulating hormone (TSH) (7). MIF transcripts and protein are also expressed in the aldosterone- and glucocorticoid-producing epithelial cells of the adrenal cortex (8), the testosterone-producing Leydig cells of the testes (9), and the insulin-secreting β cells of the pancreas (10). Furthermore, the isolation of MIF protein has been reported recently from whole bovine brain cytosol (11).

Address correspondence and reprint requests to: Dr. Richard Bucala, The Picower Institute for Medical Research, 350 Community Drive, Manhasset, NY 10021, U.S.A. Phone: 516-365-4200; Fax: 516-365-5286; E-mail: rbucala@picower.edu

To investigate more closely the role of MIF as an neuroimmunomodulator as well as its potential role in the physiology of the central nervous system, we have performed a systematic examination of MIF expression in rat brain by immunohistochemistry and in situ hybridization, both before and after the intracisternal injection of lipopolysaccharide (LPS). We report herein that MIF is expressed prominently and in a regulated fashion in rat brain parenchyma and in cerebrospinal fluid (CSF).

Materials and Methods

Animals

Male Sprague Dawley rats (250–300 grams) were obtained from Zivic-Miller Laboratories (Zelenople, PA) and were used for all experiments. The animals were maintained under strict, pathogen-free conditions and had free access to food and water.

Surgery

In-dwelling cannulae were preassembled, sterilized prior to surgery, and implanted using strict aseptic technique at Zivic-Miller Laboratories. All rats were anesthetized in a chamber supplied with a 2.5% mixture of halothane and oxygen for approximately 3–5 min, or until the proper surgical plane of anesthesia was attained. The rats then were placed on a stereotactic frame equipped with an anesthesia mask. A 1.5-cm mid-sagittal skin incision was made on the scalp to expose the skull, and the exposed area was vigorously wiped with a fresh cotton applicator to remove connective tissue. This skull was then dried and the lambda was identified. With the use of a dental drill and a No. 2 dental burr, one hole was carefully drilled through the skull at approximately 2 mm posterior and 2 mm lateral to lambda. One #0–80 stainless steel machine screw was carefully inserted so that it was seated above the dura. The incisor bar of the stereotactic frame was adjusted so that the animal's head pointed down. A small scrapper was then used to remove any muscle fibers from their point of insertion on the nuchal crest. Another hole was drilled on the midline of the nuchal crest, creating an opening between the cerebellum and the occipital squama. A sterile 28-gauge hypodermic needle was filled with artificial CSF (Harvard Apparatus, South Natick, MA) and the tip of the needle was inserted into the opening and ad-

vanced to a predetermined length for tip placement in the cisterna magnum. Cyanoacrylate glue was used to immobilize the cannula and seal the opening. The needle was attached to the skull by means of dental acrylic and was plugged with PE 20 tubing that had been heat sealed. The dental cement was allowed to harden for approximately 5 min, and the animal was released from the stereotactic frame. The rats were then injected with antibiotic and placed in a heated recovery cage. As the rats regained their righting reflex, they were removed from the heated recovery cage and housed in individual cages in an animal holding room. All procedures were in compliance with the standards recommended by the "Guide for the Care and Use of Laboratory Animals" (NIH publication No. 85-23, revised 1985). All intracisternally cannulated rats were maintained and shipped with water and normal chow ad lib.

Endotoxin Treatment

LPS (*E. coli* 0111:B4, Sigma, St. Louis, MO) was dissolved in 50 μl of artificial CSF and administered by intracisternal injection at a dose of 0.2 mg/kg. The same volume of CSF was collected through the intracisternal cannula from five animals before (0 hr), and after 3, 6, and 24 hr of LPS treatment. CSF was replaced for every time point with the same volume of artificial CSF. Alternatively, three animals were killed at the same time points following LPS administration and the brains were removed, snap-frozen in liquid nitrogen, and stored at −80°C for subsequent RNA isolation. Three control animals were injected with artificial CSF alone.

IMMUNOHISTOCHEMISTRY. Animals were sacrificed by CO_2 asphyxiation and the brains removed and fixed by immersion in 4% buffered paraformaldehyde for 24 hr. The tissues were then dehydrated in a graded series of ethanol and embedded in paraffin. The tissues were cut into 5- to 6-μm sections, mounted onto poly-L-lysine-coated glass slides, deparaffinized in xylene, and passed through decreasing concentrations of alcohol into water. The specimens were then treated in 3% H_2O_2 in phosphate-buffered saline (PBS) for 30 min in the dark to inactivate endogenous peroxidases. The sections were incubated in blocking solution (LSAB/horseradish peroxidase kit, DAKO, Botany, Australia) for 30 min and then rinsed in PBS/0.05%Tween-20.

Tissue sections were stained with a rabbit polyclonal anti-MIF antibody that was raised to purified, recombinant mouse MIF (rMIF) and affinity purified by the following procedure. Briefly, 120 μg of rMIF was electroblotted onto nitrocellulose membranes (Schleicher and Schuell, Dassel, Germany) and the membranes then cut into small pieces, transferred into glass tubes, and incubated on a shaker for 1.5 hr (25°C) with a 1:50 dilution of the rabbit, polyclonal anti-MIF serum. The bound antibodies were eluted by incubating the membrane pieces in PBS (1 ml) at 52°C for 30 min. The supernatants containing the affinity-purified anti-MIF antibodies were then removed and the process was repeated until a total of 8 ml was obtained. The solution was concentrated to a final volume of 1 ml using centrifuge concentrators, supplemented with 0.1% bovine serum albumin (BSA) and 0.02% NaN_3, and stored at 4°C until use. Control studies of rodent tissues and serum analyzed by Western blotting established that the anti-mouse MIF antibody displayed complete cross-reactivity with rat MIF, which differs from the mouse protein by only a single amino acid residue (rat MIF: Ser54, mouse MIF: Asn54) (4,12). Each section was incubated overnight at 4°C with the affinity-purified anti-MIF antibody (dilution 1:2–1:4). Antibody preabsorbed with rMIF and preimmune serum were utilized as negative controls (8). Following three washes in PBS/0.05% Tween-20, the bound antibody was visualized using the universal LSAB-2 horseradish peroxidase kit according to the manufacturer's instructions (DAKO). The sections were stained with 3-amino-9-ethylcarbazole as chromogenic substrate and counterstained with Meyer's hematoxylin. MIF expression in monocytes was examined by staining sections with an anti-CD68 antibody (ED-1, obtained from Serotec, Germany) diluted 1:200.

In Situ Hybridization

An MIF probe was prepared by first subcloning the 420 bp *Xba*/*Bam* H1 cDNA fragment into the Bluescript Sk+ vector (Stratagene, La Jolla, CA) (13). This MIF fragment is derived from the mouse MIF gene but is 100% homologous to rat MIF (4,12) and shows a single mRNA species of the predicted size when used as probe for the Northern blotting of total rat RNA (13,8). The sense and antisense MIF cRNA probes were prepared from the linearized phagemid and labeled with digoxigenin-11-UTP (Boehringer Mannheim, Germany) by in vitro transcription accord-

ing to the manufacturer's protocol. The incorporation of digoxigenin-labeled nucleotides was assayed by spotting serial dilutions of probes onto nylon membrane (Amersham, Australia) and detecting the bound probe with alkaline phosphatase-conjugated Fab fragments of anti-digoxigenin IgG with 4-nitroblue tetrazolium chloride (NBT) and X-phosphate substrates according to the manufacturer's instructions (Boehringer Mannheim, Germany). Only a probe giving detection at less than or equal to 0.1 pg/μl was used, since digoxigenin incorporation levels below this level gave poor signals in in situ hybridizations. In situ hybridization was performed on formalin-fixed, paraffin-embedded brain tissues that were cut into 4-μm thick sections and adhered to silanated, RNase-free glass slides by heating in an oven at 60°C for 1 hr. The sections were dewaxed in xylene (2 × 15 min) followed by a graded ethanol series, and rehydrated in RNase-free PBS. A newly developed microwave technique together with a conventional proteinase K treatment was used to pretreat the sections (14). Briefly, the slides were placed in a plastic slide rack and immersed inside a plastic beaker containing 300 ml of 0.01 M sodium citrate buffer (pH 6.0). The beaker was covered with polyethylene plastic wrapping and placed in the center of a microwave oven (Model MX245, Samsung, S. Korea) with an operating frequency of 2450 MHz and a power output of 900 W. The slides were heated for periods of 2 × 5 min at the maximal power setting, resulting in 140–145 sec of boiling time. The sections then were digested with 10 μg/ml proteinase K (Boehringer Mannheim, Germany) in 0.5 M NaCl/10 mM Tris-HCl buffer (pH 8.0) at 37°C for 20 min followed by treatment in 0.2 M HCl/1% Triton X-100. After washing in 2× SSC, the sections were prehybridized for 1 hr at 42°C with 0.1 ml of hybridization buffer that contained 50% deionized formamide, 4× SSC, 2× Denhardt's solution, 1 mg/ml of salmon sperm DNA (Boehringer Mannheim), and 1 mg/ml yeast tRNA. After washing in 2× SSC, the sections were incubated overnight at 42°C with 50 μl of the hybridization buffer containing 600 ng/ml of the denatured digoxigenin-labeled sense or anti-sense cRNA probe. The sections were then washed twice with 2× SSC at room temperature, followed by 0.1× SSC at 42°C. For the detection of the digoxigenin-labeled hybridized probe, the sections were first blocked with 10% normal sheep serum for 20 min and then incubated with alkaline phosphatase-conjugated, sheep anti-digoxigenin IgG for 1 hr at room temperature. The color was developed in the dark with the chromogenic agents NBT and x-phosphate and 20 mM levamisole for 3 hr. After the color was fully developed, the sections were washed, counterstained with PAS, and mounted in an aqueous solution. To make semi-quantitative comparisons between various hybridizations, all tissues were treated by exactly the same procedures and the color development was stopped at the same time (3 hr).

Two controls were employed to validate the specificity of hybridization signals. First, serial sections were hybridized with a digoxigenin-labeled sense cRNA probe at the same concentration as the corresponding anti-sense probes. Second, serial sections in which no probe was added were used to assess background staining.

DNA Amplification

Reverse transcription–polymerase chain reaction (RT-PCR) studies utilized the intron-spanning primer pairs for MIF: 5′-CCATGCCTATGTTCAT CGTG-3′ and 5′-GAACAGCGGTGCAGGTAA GTG-3′ (381 bp) (15); IL-1β: 5′-ATGTCTTGCCC GTGGAGCTT-3′ and 5′-TGTCCCGACCATTGCTG TTT-3′ (541 bp) (16); IL-6: 5′-CAAGAGACTTCC AGCCAGTTGC-3′ and 5′-TTGCCGAGTAGACC TCATAGTGACC-3′ (614 bp) (17); TNF-α: 5′-CAAAACTGCAGTGACAAGCC-3′ and 5′-GGA CTCCGTGATGTCTAAGT-3′ (423 bp) (18); β-actin: 5′-CCTGTGGCATCCATGAAACT-3′ and 5′-ATCGTACTCCTGCTTGCTGA-3′ (278 bp) (19). Each primer pair yielded the predicted size of the amplified DNA product. Frozen tissues were ground in RNAzol-B (Tel-Test Inc., Friendswood, TX) using a polytron (Littau, Switzerland) tissue homogenizer. cDNA was prepared from 0.5–1.0 μg of total RNA using 0.25 ng of oligo-(dT)12–18 and Superscript II following the manufacturer's protocol (Gibco BRL, Gaithersburg, MD). Two-microliter aliquots of cDNA then were amplified by PCR in a Perkin-Elmer model 9600 thermal cycler using the primers listed above and the following cycling program: denaturation for 1 min at 95°C, annealing for 10 sec at 55°–65°C, and extension for 20 sec at 72°C.

CSF Analysis for MIF and TNF-α

CSF samples were obtained at baseline and 3, 6, and 24 hr after the intracisternal injection of LPS. MIF content was analyzed by Western blotting using polyclonal antibodies against murine rMIF

(20). Rat TNF-α was analyzed by ELISA using a commercially available kit and following the manufacturer's protocol (Genzyme, Cambridge, MA). All samples were run in triplicate.

Results

Localization of MIF mRNA in Rat Brain

To examine first the regional and cellular localization of MIF mRNA in rat brain, sagittal sections of adult brain tissue were hybridized with a digoxigenin-labeled, antisense MIF cRNA probe. As a control, sections were also hybridized under the same conditions with a digoxigenin-labeled, sense cRNA probe. An excellent signal-to-noise ratio was obtained by this method and cell bodies hybridizing to the MIF antisense probe were detected in each of the sagittal sections that were analyzed. The most intense hybridization signals appeared to be located predominantly within neurons. Strong signals were present in the supragranular part of the cerebral cortex (Fig. 1A and C), in pyramidal neurons (regions CA1–3), in granule cells of the dentate gyrus within the hippocampus (Fig. 1E), in Purkinje cells and granular cells of the cerebellum (Fig. 2A and C), within the dorsomedial and ventromedial nuclei of the hypothalamus (Fig. 2E), in the pons (Fig. 3A), and within the plexiform and granular layer of the olfactory bulb (Fig. 3E). In the hippocampus, the cell bodies of the pyramidal cells in the CA1 to CA3 region and the granule cells of the dentate gyrus were strongly labeled, whereas the white matter showed no detectable hybridization signals (Fig. 1E). In the cerebellar cortex, a few homogeneously distributed cells within the molecular layer hybridized to the MIF probe. By contrast, intense hybridization was found in the granular layer and most prominently in the Purkinje cells (Fig. 2A and C). A much less intense but more homogenous pattern of MIF mRNA hybridization was also observed diffusely in different regions of the brain, suggesting that glial cells also express MIF in detectable levels. The specificity of the MIF hybridization signals was confirmed by performing control studies with an MIF sense cRNA probe, which demonstrated only very low levels of background staining (Fig. 4).

MIF Immunoreactivity

We used an affinity-purified antiserum raised to recombinant mouse MIF to stain sections of adult rat brains for MIF protein. Mouse MIF differs from rat MIF by only a single amino acid and this antiserum has been found in prior studies to specifically detect rat MIF protein by immunohistochemistry (8,9,21). The specificity of MIF immunostaining was established in the present study by the complete obliteration of immunopositive reactions in all regions of the brain when the MIF antiserum was preabsorbed with mouse rMIF (Fig. 5).

In contrast to the distinct appearance of MIF mRNA within the cell bodies of neurons, immunoreactive MIF protein was detected predominantly in axons. In the cerebral cortex, positive immunostaining for MIF was strongest in neuronal fibers and as a homogenous, interstitial band in the supragranular layer (Fig. 1B and 1D). At higher power, MIF protein was detected in a few dispersed cells within this same area (Fig. 1D). MIF-positive neuronal projections and terminals were observed in the hippocampus (Fig. 1F), in the hilus of the dentate gyrus and, more strongly, within the stratum lucidum in close association with the apical dendrites of pyramidal cells and the mossy fiber terminals of granule cells. A similar pattern of MIF protein immunostaining has been described recently in a study of bovine brain hippocampus (22).

A further region of intense immunoreactivity was found in the cerebellar cortex (Fig. 28 and D), most prominently in the fibers associated with Purkinje cells. Staining was less pronounced in the granular cell layer. Within the hypothalamus, the strongest staining for MIF was in the terminal fields in the ventromedial and dorsomedial nuclei. Numerous scattered cell bodies were also found to be labeled in the hypothalamus, and the homogenous pattern of staining was due most likely to glial cells. Intense immunostaining also was evident in the axonal fiber tracts of the pons (Fig. 3B), and in a few dispersed cells.

Of all regions of the brain examined, the most intense level of MIF immunostaining was in the epithelial cells of the choroid plexus (Fig. 3D). Interestingly, these cells contained no detectable MIF transcripts (Fig. 3C), suggesting that they may be involved in the uptake of MIF from the CSF.

MIF Expression after Intracisternal Endotoxin (LPS) Injection

Prior studies have identified MIF as playing a critical role in the host response to endotoxic

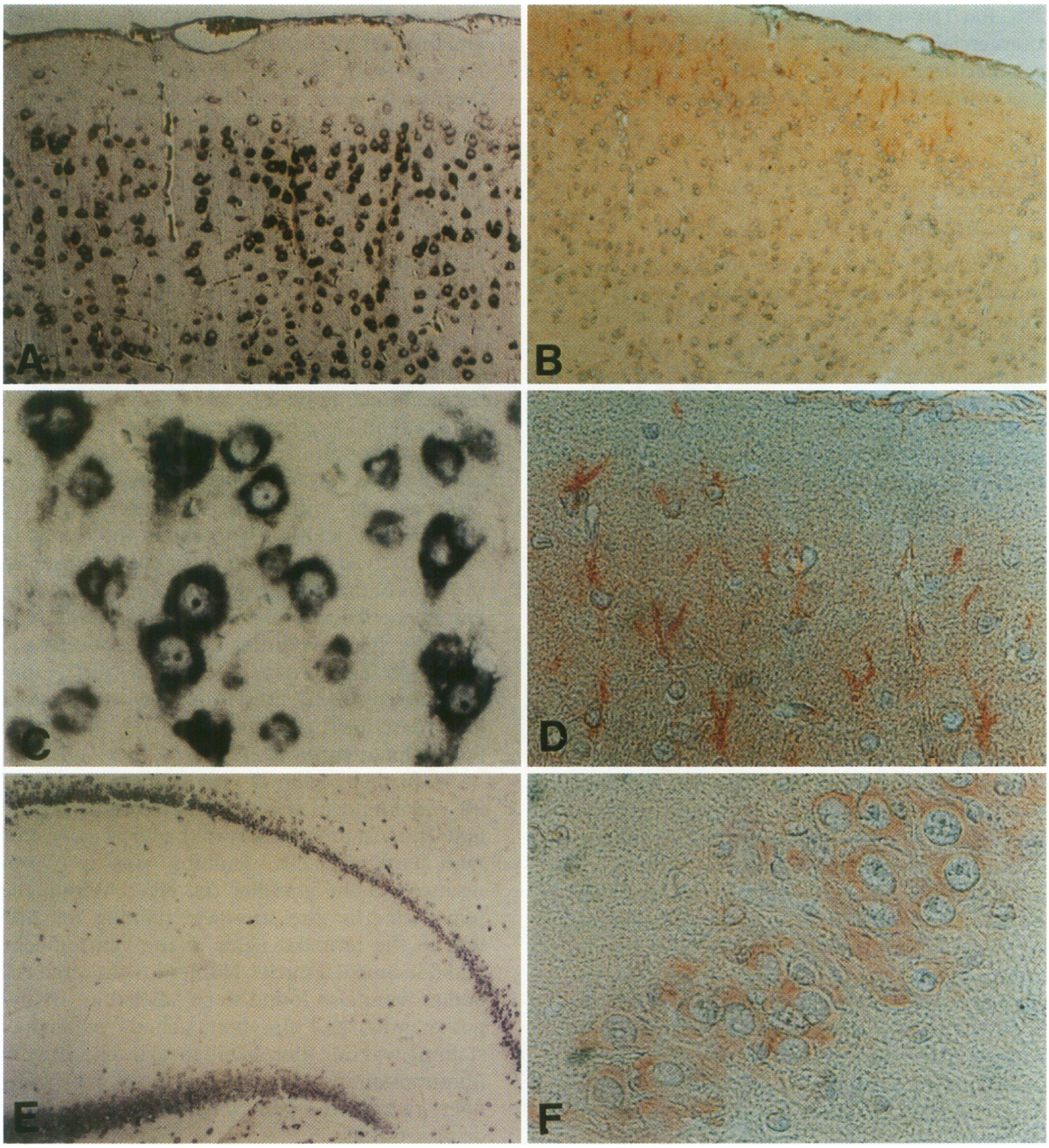

Fig. 1. MIF mRNA expression and protein immunoreactivity in the cerebral cortex (A–D) and hippocampus (E, F) of sagittal rat brain sections. (A) In situ hybridization with digoxigenin-labeled MIF cRNA probes showing strong signals in the supragranular part of the cortex (×100). (B) Immunostaining of the same region of cortex with an anti-MIF antibody (Ab) showing a consistent labeling pattern in the terminal fields of neuronal cells (×100). (C) Higher-power view of the distribution of MIF mRNA in cortex with strong hybridization signals in the cell bodies of neurons as well as in some glial cells (×400). (D) Higher-power view of MIF immunoreactivity, showing positive staining within the neuronal fiber network in the supragranular cell layer of the cortex (×200). (E) In situ hybridization for MIF mRNA in a selected section of hippocampus, with positive signals in pyramidal (CA1–CA3 field) and granule cells of the dentate gyrus (×40). (F) Immunostaining for MIF in the hippocampus, showing positive reaction within pyramidal neurons of the CA2/CA2 field (×200).

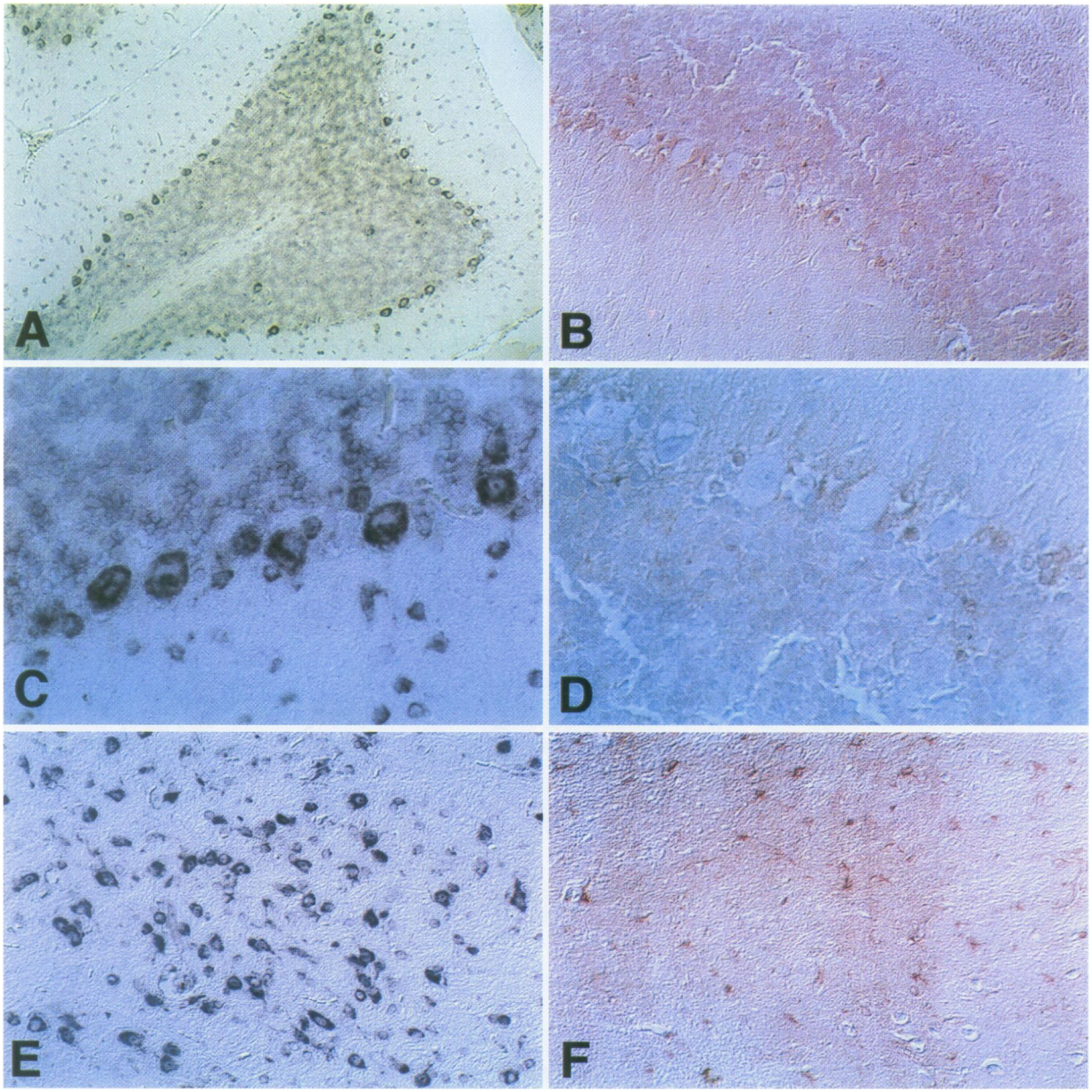

Fig. 2. MIF mRNA expression and protein immunoreactivity in the cerebellum (A–D) and hypothalamus (E, F) of the rat brain. (A) In situ hybridization showing the presence of MIF mRNA in the granular cell layer and within Purkinje cells (×100). (B) MIF immunostaining is associated with Purkinje cell projections and the granular cell layer (×100). (C) High-power view of MIF mRNA expression showing strong hybridization in the cell bodies of Purkinje cells (×400). (D) High-power view of MIF immunoreactivity in the terminal fields associated with Purkinje cells. No detectable MIF protein was evident in the cell bodies (×400). (E) MIF mRNA expression in cell bodies of the ventromedial nucleus within the hypothalamus (×200). (F) Immunostaining of the hypothalamus showing MIF protein to be distributed in the terminal fields and within scattered cell bodies (×200).

shock. The expression of MIF protein and mRNA increases in several tissue compartments as a consequence of endotoxemia, and neutralizing anti-MIF antibodies have been found to be fully protective in a mouse model of endotoxic shock (8,20). We sought to investigate the effect of endotoxin (LPS) on MIF expression in brain. Because LPS does not penetrate the intact blood-brain barrier, we administered LPS intracisternally into adult rat brains via a sterilely implanted, in-dwelling catheter. Total brain tissue was then removed at intervals and the RNA

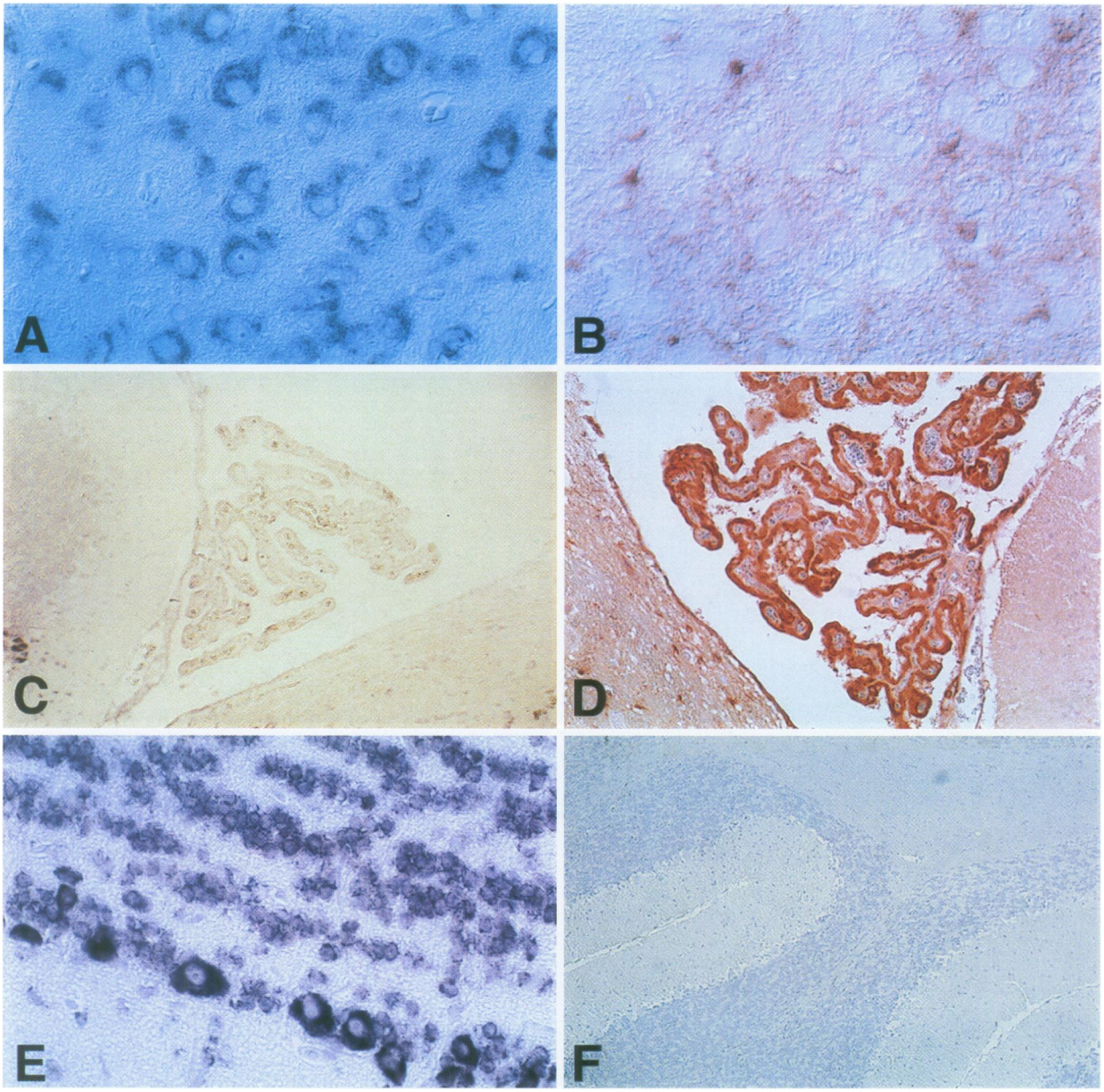

Fig. 3. MIF mRNA expression and protein immunoreactivity in the pons (A, B) choroid plexus (C, D), and within the olfactory bulb (E) of sagittal rat brain sections. (A) In situ hybridization showing the presence of MIF mRNA within the cell bodies of neurons in the pons (×400). (B) MIF immunoreactivity showing MIF protein within the terminal fields of the pons and sparing of the cell bodies (×400). (C) In situ hybridization of the choroid plexus showing very low levels of MIF mRNA hybridization in this tissue (×100). (D) Immunostaining of the choroid plexus showing strong MIF immunoreactivity within the epithelial cells (×400). (E) In situ hybridization with strong MIF mRNA expression in the cell bodies of the large neurons in the plexiform layer and in the granular layer within the olfactory bulb (×400). By contrast, no MIF protein was detectable in the olfactory bulb (data not shown). (F) Control section of cerebellum in which the primary anti-MIF antibody was preabsorbed with rMIF (×250).

isolated, reverse-transcribed, and analyzed by RT-PCR. For comparison purposes, we also examined the expression of the proinflammatory cytokines TNF-α, IL-1β, and IL-6.

Under control conditions (t = 0 hr), mRNA for MIF was readily detected at 21 cycles of DNA amplification. By contrast, the expression of mRNA for the cytokines TNFα, IL-1β, and IL-6

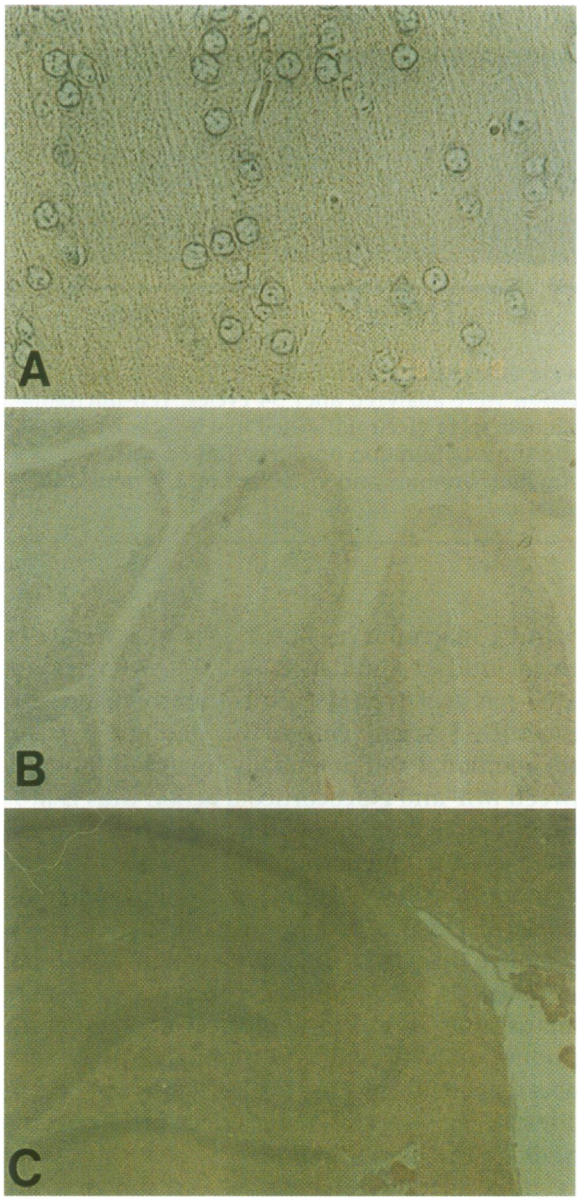

Fig. 4. Control studies examining the in situ hybridation of the MIF sense cRNA probe. Sections of cortex (A) (×400), cerebellum (B) (×100), and hippocampus (C) (×100) are shown.

was undetectable until 34 cycles, indicating that under normal conditions the mRNA for MIF is present in much more abundant quantities than these other mRNAs. This finding was confirmed by Northern hybridization in which brain RNA was sequentially hybridized with TNF-α, IL-1β, IL-6, and MIF probes. A very strong signal for MIF was observed after less than 4 hr of exposure of the Northern blot to autoradiographic film. By contrast, no signals were evident for the mRNA of the other cytokines, even after a 48-hr exposure (data not shown).

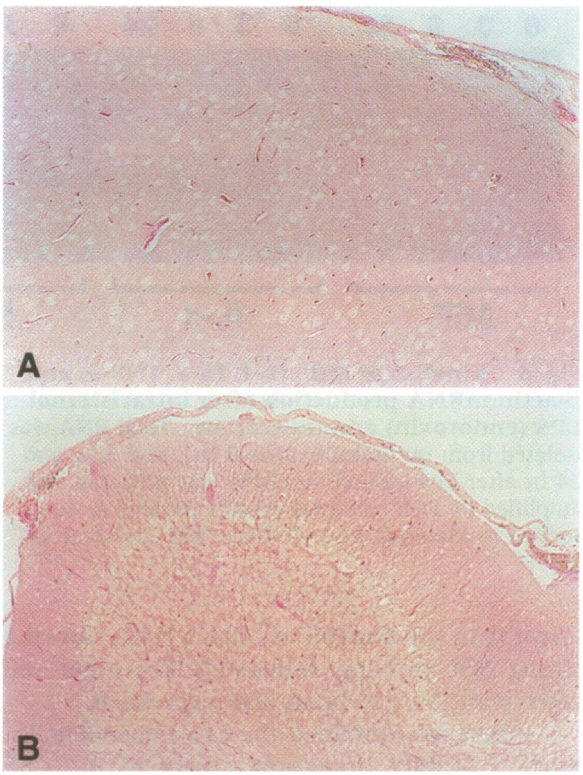

Fig. 5. Control studies examining the immunostaining of anti-MIF antibody after preabsorption with rMIF. Sections of cortex (A) (×100) and cerebellum (B) (×100) are shown.

MIF mRNA levels in brain increased after intracerebroventricular LPS administration, and reached a maximum level of induction 6 hr after endotoxin injection (Fig. 6). The mRNAs for IL-1β, IL-6, and TNF-α were detectable only after 3 hr, reached peak levels at 6 hr, and then decreased at 24 hr.

Intracerebroventricular LPS injection was also associated with the appearance of strongly positive MIF cells by immunohistochemistry (Fig. 7). MIF-labeled cells were found in the cortex (Fig. 7B) and in the hypothalamus (data not shown) within 6 hr of LPS administration, and their number increased at 24 hr (Fig. 7B, C). Staining of serial sections for the cell surface marker CD68 (ED-1) (Fig. 7G–I) revealed a portion of the MIF-positive cells to be of monocyte/macrophage origin and to be associated with blood vessel walls (Fig. 7D–F). These data indicate that infiltrating monocytes are a source of MIF-positive cells in the CNS upon LPS administration. Nevertheless, the LPS-dependent induction of MIF within the rat brain is not entirely due to blood monocyte infiltration since the number of ED-1-positive cells was substantially

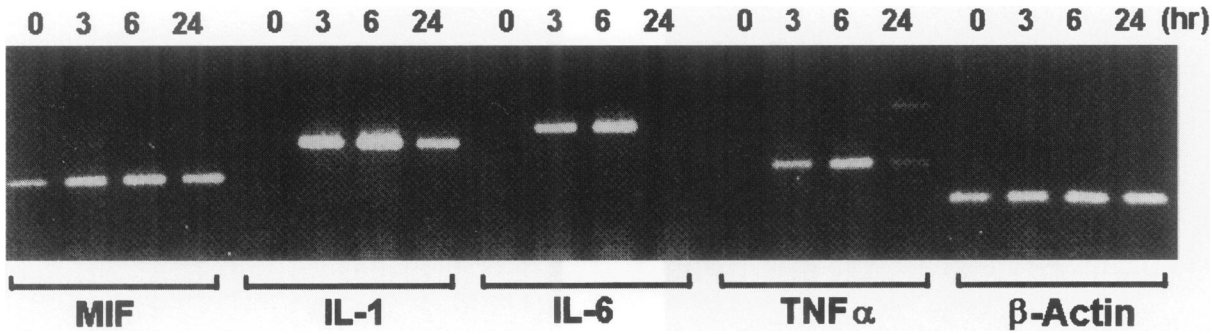

Fig. 6. Kinetics of MIF, IL-1, IL-6, TNF-α, and β-actin mRNA production after intracisternal LPS (endotoxin) administration. Total RNA was isolated from rat brains before (0 hr), and 3, 6, and 24 hr after LPS treatment. cDNA was prepared and amplified by PCR using rat specific primers as described in Materials and Methods. MIF and β-actin were analyzed after 21 cycles, IL-1β, IL-6, and TNF-α were analyzed after 34 cycles. Ten-microliter aliquots were electrophoresed in 1% agarose gels and the amplification products stained with ethidium bromide and visualized by UV transillumination.

lower than the number of cells in brain showing strong MIF staining, indicating that other cell types contribute to brain MIF expression.

When we examined the LPS-dependent induction of MIF immunoreactivity in the CSF (Fig. 8), we observed a sharp peak of MIF immunoreactivity after 3 hr of LPS injection. The magnitude of the inflammatory response correlated with the induction of TNF-α. In a group of five tested animals, the lowest and the highest levels of MIF induction were accompanied by a corresponding pattern of TNF-α expression (Fig. 8).

Discussion

We have examined the complete regional and cellular distribution of MIF mRNA and protein in the adult rat brain. The high abundance of MIF mRNA and protein that is associated with different neurons suggests a requirement for this protein in aspects of CNS physiology that include autonomic, hypophysiotrophic, limbic, and extrapyramidal functions. The occurrence of MIF within the hypothalamus also complements prior studies identifying MIF as an important molecular constituent of the HPA axis. MIF is released by stress from the corticotrophic cells of the anterior pituitary gland (20,7), and it also is present preformed within the zona glomerulosa of the adrenal gland. Both the pituitary and the adrenals secrete MIF in the course of a systemic inflammatory response induced by endotoxemia (7,8).

Within the immune system, MIF is secreted both by macrophages and T cells in response to glucocorticoid stimulation (6,23). Once released, MIF acts to "override" or counterregulate glucocorticoid action within the immune system. An additional and potentially important link between MIF and glucocorticoid action thus is provided by the finding of prominent MIF expression in the hippocampus. Damage to the hippocampus has been linked to high circulating levels of glucocorticoids. In particular, there is evidence to suggest that an elevation in adrenal steroids—as occurs during chronic stress—may induce long-term morphological alterations including atrophy and a permanent loss of hippocampal neurons (24–27). MIF thus may act to directly regulate this toxic effect of glucocorticoids on the hippocampus.

Glucocorticoids have also been shown to act synergistically with various excitatory amino acids (28,29). Mossy fibers originating from the granule cells of the dentate gyrus provide a strong input of excitatory amino acids into the hippocampal CA3 region (30). MIF immunoreactivity was associated with mossy fibers, as well as with the dendritic branches of the hippocampal CA3 field, a second area that has been described to suffer from glucocorticoid-induced atrophy (26,27).

Although a precise functional relationship between MIF and glucocorticoid action in the brain remains to be experimentally established, it should be noted that there are also recent data linking MIF expression with the local regulation of various endocrine tissues. In the testes, Leydig cell MIF production has been found to regulate inhibin secretion by Sertoli cells (9), and within

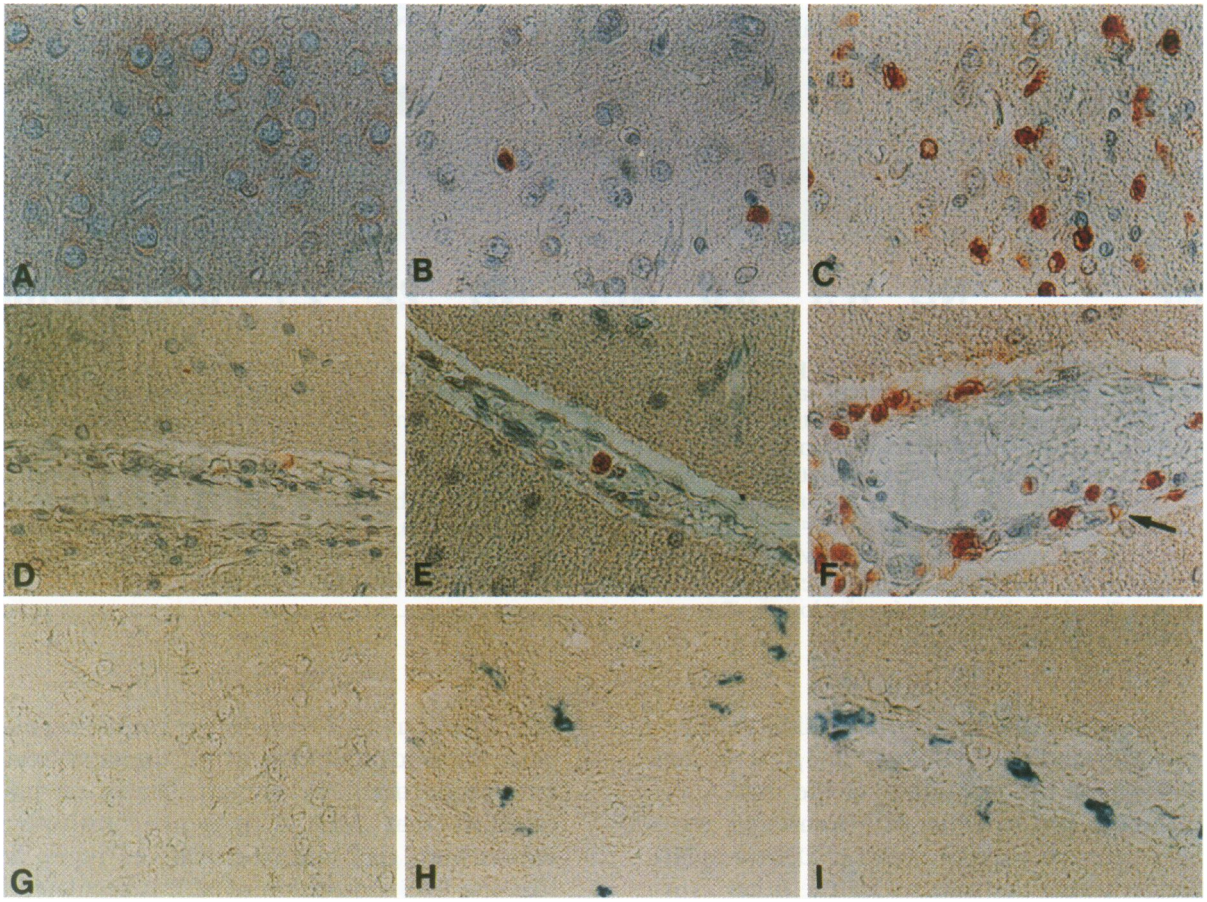

Fig. 7. Evidence of MIF-positive cells by immunohistochemistry. MIF immunoreactivity in the cerebral cortex (A–C) and in blood vessels (D–F) in untreated rats (A, D), and 6 hr (B, E) and 24 hr (C, F) after LPS injection. Immunostaining for ED1-positive monocytes in the cortex (G, H) and blood vessels (I) in untreated rats (G), and 24 hr after LPS administration (H, I) (×400).

the β cells of the endocrine pancreas, MIF secretion regulates the glucose-dependent release of insulin (10).

We found that there was a significant discrepancy between the expression of MIF mRNA and protein in the olfactory bulb. A strong hybridization signal for MIF mRNA was evident but no MIF immunoreactivity could be detected. Possible explanations for this result might be a fast axonal transport and release of MIF, or that MIF might bind to a locally produced factor in the olfactory bulb which abolishes antibody recognition.

Outside of neurons and their processes, MIF mRNA and proteins were also detected diffusely throughout the brain, suggesting that glial cells were also a source of MIF expression. This complements the recent identification of MIF as an important secretory component of monocytes and tissue macrophages (5,8).

We also examined the effect of intracisternal LPS administration on MIF mRNA and protein expression. It is worth noting that the regional and cellular distribution of MIF at baseline showed certain similarities with what has been described previously for the cytokines IL-1β and IL-6. (31–35). The mRNAs for IL-1β and IL-6 are also present in the cell bodies of hippocampal and cerebellar neurons, and immunoreactive IL-1β can be detected within the neuronal processes and terminals of pyramidal and granular cells within the hippocampus. Infiltrating monocytes, in part associated with the walls of blood vessels, are another source of LPS-induced MIF and cytokine production in the CNS. As expected, intracisternal LPS injection was associated with a significant increase in the expression of mRNAs encoding MIF, IL-1β, IL-6, and TNF-α (36,37). The level of MIF mRNA did not appear to increase as significantly as for the other cyto-

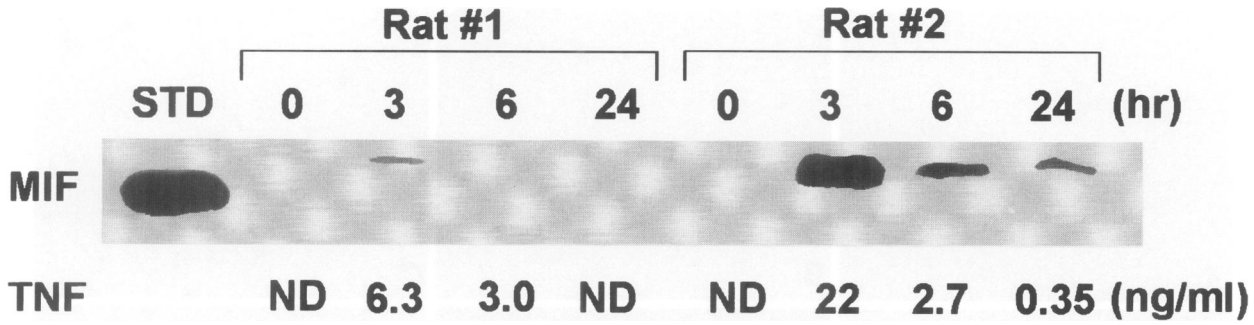

Fig. 8. Kinetics of MIF and TNF-α production in the CSF of rats after intracisternal LPS injection. CSF aliquots (50 μl) were collected before (0 hr), and 3, 6, and 24 hr after endotoxin treatment. Samples were analyzed by Western blotting (MIF) or by ELISA (TNF-α) as described in Materials and Methods. The numerical values for TNF-α content are depicted below the corresponding MIF bands for each time point. The ELISA samples were run in triplicate. The data shown are for the lowest (Rat #1) and highest (Rat #2) responders in an experimental group of five animals. ND: not detected. Mean ± SD and p values by two-tailed Student's T test: Rat #1, 3 hr: 6.30 ± 0.08 ng/ml, 6 hr: 3.05 ± 0.13 ng/ml; $p = 0.006$ for 3 hr vs. 0 hr, $p = 0.019$ for 6 hr vs. 0 hr. Rat #2, 3 hr: 22.64 ± 0.91 ng/ml, 6 hr: 2.66 ± 0.18 ng/ml, 24 hr: 0.35 ± 0.06 ng/ml; $p = 0.018$ for 3 hr vs. 0 hr, $p = 0.019$ for 6 hr vs. 0 hr, $p = 0.077$ for 24 hr vs. 0 hr.

kines. However, the most striking difference between MIF and the cytokines IL-1β, IL-6, and TNF-α was in the magnitude of the mRNA expression level at baseline. MIF transcripts were readily detected after 21 cycles of DNA amplification, whereas the mRNAs for the other cytokines were not detectable until 34 cycles. From our experience with these primer sequences, this result implies at least a 4-log difference in baseline expression levels. These data are also consistent with results obtained by Northern blotting analysis of whole rat brains (M. Bacher et al., unpublished observations).

Intracisternal LPS administration was also associated with the appearance of MIF protein in the CSF. The increase in MIF in this compartment was due most likely to MIF release from the epithelial cells of the choroid plexus. At baseline, these cells showed the strongest immunoreactivity for MIF among the brain structures that were examined. Interestingly, the choroid plexus showed very little MIF mRNA by in situ hybridization, suggesting that this tissue plays a role in the uptake or transport of MIF. LPS, either directly or via secondary mediators, may then induce the release of MIF from the epithelial cell pool. The magnitude of MIF release into the CSF also correlated with the magnitude of the LPS-induced TNF-α response.

Recent studies have identified MIF as both an anterior pituitary hormone and an immune cell "cytokine" released in response to glucocorticoid stimulation. Within the immune system, MIF functions to "override" or counterregulate glucocorticoid inhibition of inflammatory cytokine production. The present data in rat brain establish that MIF is present constitutively within both glial and neuronal cell types, and that the CNS expression of MIF is regulated by inflammatory stimuli such as LPS. MIF may function as a neuromodulator, neurotransmitter, or neurotrophic factor, and it may be associated with glucocorticoid action within the CNS. The high levels of baseline and inducible MIF expression in the brain nevertheless underscore its role as a neuroendocrine mediator and extend the importance of MIF as a physiological regulator of the inflammatory stress response.

Acknowledgments

This work was supported by NIH grant A135931 and NH&MRC960106.

References

1. George M, Vaughan JH. (1962) In vitro cell migration as a model for delayed hypersensitivity. *Proc. Soc. Exp. Biol. Med.* **111:** 514–521.
2. Bloom BR, Bennett B. (1966) Mechanism of a reaction in vitro associated with delayed-type hypersensitivity. *Science* **153:** 80–82.
3. David JR. (1966) Delayed hypersensitivity in vitro: Its mediation by cell free substances formed by lymphoid cell-antigen interaction. *Proc. Natl. Acad. Sci. U.S.A.* **56:** 72–77.

4. Bernhagen J, Mitchell RA, Calandra T, Voelter W, Cerami A, Bucala R. (1994) Purification, bioactivity, and secondary structure analysis of mouse and human macrophage migration inhibitory factor (MIF). *Biochemistry* **33:** 14144–14155.
5. Calandra T, Bernhagen J, Mitchell RA, Bucala R. (1994) The macrophage is an important and previously unrecognized source of macrophage migration inhibitory factor. *J. Exp. Med.* **179:** 1895–1902.
6. Calandra T, Bernhagen J, Metz CN, Spiegel LA, Bacher M, Donnelly T, Cerami A, Bucala R. (1995) MIF is a glucocorticoid-induced modulator of cytokine production. *Nature* **377:** 68–71.
7. Nishino T, Bernhagen J, Shiiki H, Calandra T, Dohi K, Bucala R. (1995) Localization of macrophage migration inhibitory factor (MIF) to secretory granules within the corticotrophic and thyrotrophic cells of the pituitary gland. *Mol. Med.* **1:** 781–788.
8. Bacher M, Meinhardt A, Lan HY, Wei Mu, Metz CN, Chesney JA, Calandra T, Gemsa D, Atkins RC, Bucala R. (1997) MIF expression in experimentally induced endotoxemia. *Am. J. Pathol.* **150:** 235–246.
9. Meinhardt A, Bacher M, McFarlane JR, Metz CN, Seitz J, Hedger MP, De Kretser, DM, Bucala R. (1996). Macrophage migration inhibitory factor production by Leydig cells: Evidence for a role in the regulation of testicular function. *Endocrinology* **137:** 5090–5095.
10. Waeber G, Calandra T, Roduit R, Haefliger J-A, Thompson N, Thorens B, Temler E, Meinhardt A, Bacher M, Metz CN, Nicod P, Bucala R. (1997) Insulin secretion regulated by the glucose dependent production of islet β-cell MIF. *Proc. Natl. Acad. Sci. U.S.A.* **94:** 4782–4787.
11. Galat A, Riviere S, Bouet F. (1993) Purification of macrophage migration inhibitory factor (MIF) from bovine brain cytosoll. *FEBS Lett.* **319:** 233–236.
12. Sakai M, Nishihira J, Hibiya Y, Koyama Y, Nishi S. (1994) Glutathione binding rat liver 13k protein is homologous of the macrophage migration inhibitory factor. *Biochem. Mol. Biol. Int.* **33:** 439–446.
13. Mitchell R, Bacher M, Bernhagen J, Pushkarskaya T, Seldin M, Bucala, R. (1995) Cloning and characterization of the gene for mouse macrophage migration inhibitory factor (MIF). *J. Immunol.* **154:** 3863–3870.
14. Lan HY, Mu W, Ng Y, Nikolic-Paterson DJ, Atkins RC. (1996) A simple, reliable, and sensitive method of nonradioactive in situ hybridization: Use of microwave heating to improve hybridization efficiency and preserve tissue morphology. *J. Histochem. Cytochem.* **44:** 281–287.
15. Bernhagen J, Bacher M, Calandra T, Metz CN, Doty SB, Donnelly T, Bucala R. (1995) An essential role for macrophage migration inhibitory factor (MIF) in the tuberculin delayed-type hypersensitivity reaction. *J. Exp. Med.* **183:** 277–282.
16. Feeser W, Freimark BD. (1992) Genebank accession #M98820.
17. Northemann W, Braciak TA, Hattori M, Lee F, Fey GH. (1989) Structure of the rat interleukin 6 gene and its expression in macrophage derived cells. *J. Biol. Chem.* **264:** 16072–16082.
18. Shirai T, Shimizu N, Horiguchi S, Ito H. (1989) Cloning and expression in *Escherichia coli* of the gene for rat tumor necrosis factor. *Agric. Biol. Chem.* **53:** 1733–1736.
19. Nudel U, Zakut R, Shani M, Neumann S, Levy Z, Yaffe D. (1986) The nucleotide sequence of the rat cytoplasmic beta-actin gene. *Nucl. Acids Res.* **11:** 1759–1771.
20. Bernhagen J, Calandra T, Mitchell RA, Martin SB, Tracey KJ, Voelter W, Manogue KR, Cerami A, Bucala R. (1993) MIF is a pituitary-derived cytokine that potentiates lethal endotoxemia. *Nature* **365:** 756–759.
21. Lan HY, Mu W, Yang N, Meinhardt A, Nikolic-Paterson DJ, Ng YY, Bacher M, Atkins RC, Bucala R. (1996) De novo renal expression of macrophage migration inhibitory factor during the development of rat crescentic glomerulonephritis. *Am. J. Pathol.* **149:** 1119–1127.
22. Nishibori M, Nakaya N, Tahara A, Kawabata M, Mori S, Saeki K. (1996) Presence of macrophage migration inhibitory factor (MIF) in ependyma, astrocytes and neurons in the bovine brain. *Neurosci. Lett.* **213:** 193–196.
23. Bacher M, Metz, CN, Calandra T, Mayer K, Chesney J, Lohoff M, Gemsa D, Donnelly T, Bucala R. (1996) An essential regulatory role for MIF in T-cell activation. *Proc. Natl. Acad. Sci. U.S.A.* **93:** 7849–7854.
24. Uno H, Tarara R, Else JG, Suleman, MA, Sapolsky RM. (1989) Hippocampal damage associated with prolonged and fatal stress in primates. *J. Neurosci.* **9:** 1705–1711.
25. Sapolsky RM, Uno H, Rebert CS, Finch CE. (1990) Hippocampal damage associated with prolonged glucocorticoid exposure in primates. *J. Neurosci.* **10:** 2897–2902.
26. Wooley CS, Gould E, McEwen BS. (1990) Exposure to excess glucocorticoids alters dendritic morphology of adult hippocampus pyramidal neurons. *Brain Res.* **531:** 225–231.
27. Magarinos AM, McEwen BS, Fluegge G, Fuchs E. (1996) Chronic psychosocial stress causes apical dendritic atrophy of hippocampal CA3 pyramidal neurons in subordinate tree shrews. *J. Neurosci.* **16:** 3534–3540.
28. Krugers HJ, Koolhaas JM, Bohus B, Korf J. (1993) A single social stress experience alters glutamate receptor-binding in rat hippocampal CA3 area. *Neurosci. Lett.* **154:** 73–77.
29. Lowy MT, Gault L, Yamamoto BK. (1993) Adre-

nalectomy attenuates stress-induced elevation in extracellular glutamate concentrations in the hippocampus. *J. Neurochem.* **61:** 1957–1960.
30. Clairbone BJ, Amaral DG, Cowan WH. (1986) A light microscopy analysis of the mossy fibers of the rat dentate gyrus. *J. Comp. Neurol.* **246:** 435–458.
31. Bandtlow CE, Meyer M, Lindholm D, Spranger M, Heumann R, Thoenen H. (1990) Regional and cellular codistribution of interleukin-1β and nerve growth factor mRNA in the adult rat brain: Possible relationship to the regulation of nerve growth factor synthesis. *J. Cell. Biol.* **111:** 1701–1711.
32. Lechan RM, Clark TBD, Cannon JG, Shaw AR, Dinarello CA, Reichlin S. (1990). Immunoreactive interleulin-1β localization in the rat forebrain. *Brain Res.* **514:** 135–140.
33. Schoebitz B, Voorhuis DAM, De Kloet ER. (1992) Localization of interleukin 6 mRNA and interleukin 6 receptor mRNA in rat brain. *Neurosci. Lett.* **136:** 189–192.
34. Yan HQ, Banos MA, Herregodts P, Hooghe R, Hooghe-Peters EL. (1992) Expression of interleukin (IL)-1β, IL-6 and their respective receptors in the normal rat brain and after injury. *Eur. J. Immunol.* **22:** 2963–2971.
35. Gadient RA, Otten U. (1994) Identification of interleukin-6-expressing neurons in the cerebellum and hippocampus of normal adult rats. *Neurosci. Lett.* **182:** 243–246.
36. Higgins GA, Olschowaka JA. (1991) Induction of interleukin-1 beta mRNA in adult rat brain. *Mol. Brain Res.* **9:** 143–148.
37. Hunter CA, Roberts CW, Alexander J. (1992) Kinetics of cytokine mRNA production in the brain of mice with progressive toxoplasmic encephalitis. *Eur. J. Immunol.* **22:** 2317–2322.